

College of Saint Benedict and Saint John's University

DigitalCommons@CSB/SJU

Celebrating Scholarship & Creativity Day

Experiential Learning & Community
Engagement

4-23-2015

Photometric Extraction of the Pulse and Orbital Periods of ASAS182612: Eclipsing Binary with a Type II Cepheid Component

Joseph E. Hoppert

College of Saint Benedict/Saint John's University

Follow this and additional works at: https://digitalcommons.csbsju.edu/elce_cscday



Part of the [Physics Commons](#)

Recommended Citation

Hoppert, Joseph E., "Photometric Extraction of the Pulse and Orbital Periods of ASAS182612: Eclipsing Binary with a Type II Cepheid Component" (2015). *Celebrating Scholarship & Creativity Day*. 69.

https://digitalcommons.csbsju.edu/elce_cscday/69

This Presentation is brought to you for free and open access by DigitalCommons@CSB/SJU. It has been accepted for inclusion in Celebrating Scholarship & Creativity Day by an authorized administrator of DigitalCommons@CSB/SJU. For more information, please contact digitalcommons@csbsju.edu.

PHOTOMETRIC EXTRACTION OF THE PULSE AND ORBITAL PERIODS OF ASAS182612:
ECLIPSING BINARY WITH A TYPE II CEPHEID COMPONENT

UNDERGRADUATE THESIS
College of St. Benedict/St. John's University
In Partial Fulfillment
Of the Requirements for Distinction
in the Department of Physics
by
Joseph E. Hoppert
May 2015

Abstract

In 2007, Antipin, Sokolovsky, and Ignatieva discovered the first eclipsing binary with a Type II Cepheid component in our Galaxy, ASAS182612. We present the analysis of ASAS182612's pulse and orbital periods from 2007 to 2014 using B, V, R, and I filters. The pulsation and orbital periods were found to be $4.1622 \pm .0003$ days and $51.366 \pm .025$ days, respectively. The angular acceleration of the pulse period was determined to be $1.1\text{E-}6 \pm 1\text{E-}7$ rad/day².

Table of contents

Introduction.....	4
Theory.....	6
Magnitude.....	6
Color.....	6
Color Correction.....	6
Truncated Fourier Series.....	7
Pulse and Orbital Periods.....	8
Missing Light.....	9
Methods.....	10
Detector System.....	10
Camera/Filters.....	10
Programs/Software.....	12
Initialization.....	13
Flat Frames.....	13
Dark Frames.....	14
Focus.....	15
IC4665 CCD Frames for Calibration.....	15
ASAS182612 CCD Frames.....	16
Data Frames.....	17
Data/Analysis.....	19
Gaia Collection of Star Magnitudes.....	19
Color Correction.....	19
Download AAVSO ASAS182612 Magnitude Data.....	20
Condense AAVSO Data.....	20
Mathematica Chauvenet Criteria and Fit Functions on AAVSO Data.....	20
AAVSO Pulse and Orbital Periods.....	22
Download SJU ASAS182612 Magnitude Data.....	23
Mathematica Fit Functions with Angular Acceleration on SJU Data.....	23
SJU Pulse and Orbital Periods.....	25
SJU Angular Acceleration of the Pulse Period.....	27
SJU Missing Light of ASAS182612.....	28
Conclusions.....	30
Acknowledgements.....	31
References.....	32

1 Introduction

In 2007, Antipin, Sokolovsky, and Ignatieva discovered the first eclipsing binary with a Type II Cepheid component in our Galaxy, ASAS182612. The variability was discovered by the astronomers on Moscow archive plates taken with the 40-cm astrograph in Crimea (Antipin, Sokolovsky, & Ignatieva 2007). The photographic phased light curves, produced by their independent research, concluded that this new variable could be considered a Cepheid with some peculiarity similar to multiperiodicity. Since the available data could not fully explain the observed variations of light, observations of ASAS182612 were started in 2004 with the 50-cm Maksutov telescope of the Crimean Laboratory (Sternberg Astronomical Institute) equipped with a Pictor 416XTE CCD camera and Johnson V filter. These observations continued for three years: 729 images on 17 nights in 2004 (July 4–29, JD2453191–216), 560 images on 13 nights in 2005 (July 1–19, JD2453553–571), and additional 367 images on 24 nights in 2006 (July 4 – August 2, JD2453921–950) were obtained (Antipin, Sokolovsky, & Ignatieva 2007).

From their V-band analysis of ASAS182612, the astronomers were able to classify the binary system as a Type II Cepheid. However, their detection of eclipses and observations in the V filter was just the first step in the investigation of this unique star system. The Type II Cepheid, eclipsing, and ellipsoidal components of ASAS182612 make it a unique celestial object. The Cepheid component of the binary system relates to the star's radial pulsation, varying between a larger, brighter state and a smaller, denser state usually with a well-defined stable period (Percy 2007). During an eclipse the star dims thus yielding an increase in the apparent magnitude. Lastly, the ellipsoidal component of the variable causes changes in the apparent brightness caused by mutual gravitational forces of the stars in the binary system, which deforms the stars

from a spheroidal shape. When we see the elongated star from the side there is more incandescent area and hence a brighter star.

Here we continue observations of the variable star presenting the results of multi-filter photometric extraction of the pulse and orbital periods of ASAS182612.

2 Theory

Magnitude:

Astronomers typically measure light in magnitudes. Magnitudes are related to flux by:

$$m = -2.5 \log_{10} \left(\frac{F}{F_0} \right) \quad (1)$$

where F_0 is the standardizing flux corresponding to $m=0$. The negative sign in Equation 1 displays how magnitudes work: the brighter the star, the smaller the magnitude and vice versa. However, magnitude is not an intrinsic property of a star because the measured flux of a star depends on distance.

Color:

At increasing distance from the star relative fluxes of F_λ will diminish by the same fraction. The ratio of two fluxes measured in different wavelengths is an intrinsic property of the star. This ratio is a measure of the relative amounts of two colors, and as such is called a color index (Kirkman 2013). The most common color index is B-V, which can be calculated from the following equation:

$$B - V = 2.5 \log \left(\frac{F_V}{F_B} \right) + constant \quad (2)$$

where B-V is the color index of the B and V magnitudes of the observed object and F_B and F_V are the respective flux values for the B and V filters.

Color Correction:

Earth's atmosphere and the entire detection system are analogous to a non-negligible colored filter, attenuating starlight before it reaches the telescope. The simple fact that the atmosphere looks blue and the setting Sun look red tells us that it acts as a colored filter, scattering and

attenuating some wavelengths more than others. This implies that two stars, outside the Earth's atmosphere having the same magnitude but different temperatures, will measure having different magnitudes from the Earth's surface. The atmospheric optical depth parameter τ_0 , depends slightly on the temperature, T , of the star:

$$B = 2.5\tau_0(T) \log_{10}(e) \sec(z) + B_0 \quad (3)$$

where B is the magnitude through the B filter at ground level and B_0 is the atmosphere-free B magnitude. The temperature of the star is related to the actual B_0-V_0 color index, which in turn is related to the instrumental color index $b-v$ (Kirkman 2013). Making a first order Taylor series expansion of $\tau_0(T)$ in terms of $b-v$, we have:

$$b \approx \alpha_B + \beta_B(b - v) + B_0 \quad (4)$$

This is the offset between the instrumental magnitude and the atmosphere-free magnitude. A linear fit (using the data from the calibrated sources) can be used to solve for α and β :

$$b - B_0 = \alpha_B + \beta_B(b - v) \quad (5)$$

and similarly for V magnitudes:

$$v - V_0 = \alpha_V + \beta_V(b - v) \quad (6)$$

Subtracting these two magnitude equations yields the relationship between the instrumental color index and the atmosphere-free color index:

$$(b - v) - (B_0 - V_0) = \alpha_B - \alpha_V + (\beta_B - \beta_V)(b - v) \quad (7)$$

$$[1 + (\beta_V - \beta_B)](b - v) + (\alpha_V - \alpha_B) = B_0 - V_0 \quad (8)$$

Thus between the instrumental color index and atmosphere-free color index we expect a linear relationship. The parameters of this linear relationship can be determined by a fit using the data from the calibrated stars.

Truncated Fourier Series:

A Fourier series is a way to represent any periodic function or signal as an infinite sum of a set

of simple oscillation functions such as sines and cosines. Here a truncated Fourier series simply cuts off the infinite summation of the Fourier series where only the statistically significant components are used. The typical Fourier series can be represented by:

$$F(x) = b_0 + \sum_{n=1}^{\infty} a_n \sin(n a x) + \sum_{n=1}^{\infty} b_n \cos(n a x) \quad (9)$$

Pulse and Orbital Periods:

A stars pulse period is directly related to the stars fundamental angular frequency a :

$$\tau_P = \frac{2\pi}{a} \quad (10)$$

$$\delta\tau_P = \frac{\left| \frac{2\pi}{a_{lower}} - \frac{2\pi}{a_{upper}} \right|}{2} \quad (11)$$

where the value of a is determined from a fit to the data. The uncertainty in the pulse period can be found from the lower and upper confidence intervals of a , a_{lower} and a_{upper} respectively, which are supplied by the fitting program.

Ellipsoidal and eclipsing variable stars are components of close binary systems. In ellipsoidal variables, the shape of each star is distorted by its companion. This causes the brightness of the star to be non-uniform. The eclipsing variables tend to vary the brightness as one star periodically eclipses the other, in a binary system, producing a change in the brightness by geometrical effect. The stars therefore change their apparent brightness, with a period equal to half orbital period, because of changes in the brightness and projected emitting area turned to the observer. The orbital period of the variable can be determined by:

$$\tau_O = \frac{4\pi}{b} \quad (12)$$

$$\delta\tau_O = \frac{\left| \frac{4\pi}{b_{lower}} - \frac{4\pi}{b_{upper}} \right|}{2} \quad (13)$$

where the value of b is determined by a fit including a magnitude variation of form:

$$A \sin(b t) + B \cos(b t) \quad (14)$$

The uncertainty in the orbital period can be found from the lower and upper confidence intervals

of b , b_{lower} and b_{upper} respectively.

Missing Light:

The missing light of a variable star corresponds to the unobservable light of the variable during an eclipse in a binary system. This unobservable light can be calculated by determining the seen light and expected light and using the equation of the following form:

$$M_{unseen} = -2.5 \log_{10} \left(10^{-\frac{M_{expected}}{2.5}} - 10^{-\frac{M_{seen}}{2.5}} \right) \quad (15)$$

where M is the magnitude of light through a B, V, R, or I filter.

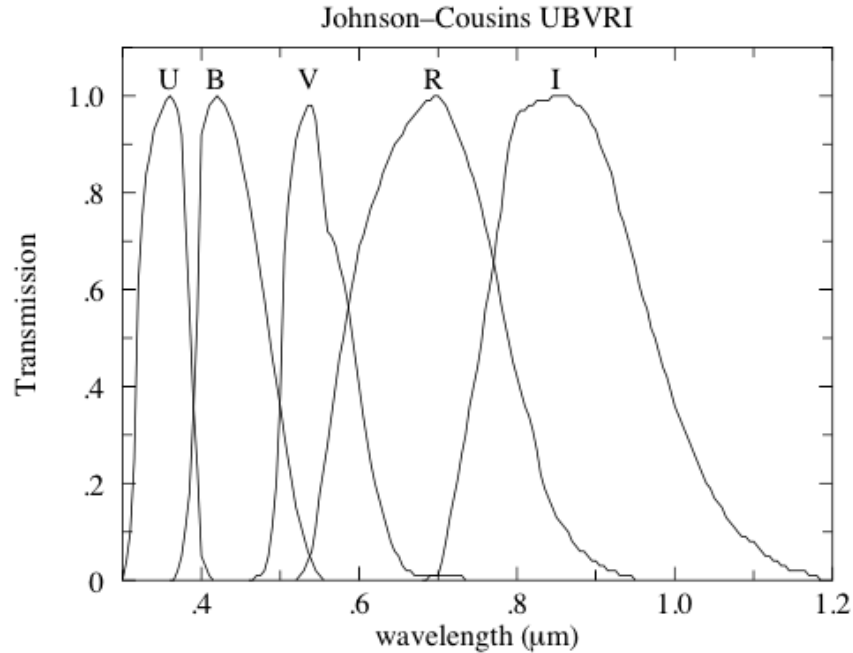
3 Methods:

Detector system:

Camera/Filters

Photons were counted using a charge coupled device (CCD). The image sensor, Kodak KAF-1001E CCD, consists of a 26-pin Dual In-line Package (DIP) integrated circuit with a 1"x1" window that exposes 1024x1024 pixels to incident light. The photons incident on a pixel free electrons via the photoelectric effect during an exposure. Each pixel stored a charge during an exposure and then the charge was transferred to a capacitor where it produced a voltage, which is proportional to the number of electrons. An Analog-to-Digital converter (ADC) then converted the voltage to a 16-bit binary number to create an "image" consisting of a 1024x1024 matrix of integers measured in Analog-to-Digital Units (ADU). From the combined effects of photon quantum efficiency and ADU gain there are approximately four incident photons per ADU count.

The Kodak CCD was controlled by a STL-1001E camera built by the Santa Barbara Instrument Group. In front of the camera, a SBIG FW8-STL filter wheel allows for software controlled switching between B, V, R, I, g', r', i' filters or a null (blank) filter. Much of astronomy revolves around observations made through the five standard U, B, V, R, and I filters. Each filter essentially allows transmission for a range of wavelengths $\Delta\lambda$, centered on a particular wavelength, where the characteristics of these filters are displayed in Figure 1. The name of the filter is related to the type of light that is allowed to pass through the filter: U (ultraviolet), B (blue), V (visible or green), R (red), and lastly I (infrared). Here we were only concerned with the B, V, R, and I filters for data collection.



Filter Name	λ (μm)	$\Delta\lambda$ (μm)	F_0 ($\text{W}/\text{m}^2 \mu\text{m}$)
<i>U</i>	0.36	0.07	4.22×10^{-8}
<i>B</i>	0.44	0.10	6.40×10^{-8}
<i>V</i>	0.55	0.09	3.75×10^{-8}
<i>R</i>	0.71	0.22	1.75×10^{-8}
<i>I</i>	0.97	0.24	0.84×10^{-8}

Figure 1: Characteristics of the standard filters: U (ultraviolet), B (blue), V (visible), R (red), I (infrared) from *Allen's Astrophysical Quantities* p. 387 and The General Catalogue of Photometric Data: <http://obswww.unige.ch/gcpd/system.html>

The SBIG camera is mounted on a Meade 12" LX200 Schmidt-Cassegrain Catadioptric telescope. After the telescope has been initialized, the telescope control software (TheSkyX) from Software Bisque can direct the telescope to cataloged objects or most any direction above the horizon. Figure 2 displays the detailed CCD photometry equipment list used at the St. John's University observatory.

Photometry

Telescope	Meade LX200	CCD	Kodak KAF-1001E
aperture	12"	pixel	24 μm \times 24 μm
focal ratio	$f/10$	full-well	$\sim 150,000 e^-/\text{pixel}$
focal length	120"	read noise	15 e^- rms
		gain	2.03 e^-/ADU
Filter Wheel	SBIG FW8-STL		
filters	blank, $BVRI$, $g'r'i'$	λ	Quantum Efficiency
Camera	SBIG ST-1001E NABG	.95 μm	20%
pixels	1024 \times 1024	.80 μm	50%
image	28' \times 28'	.65 μm	65%
scale	1.65"/pixel	.50 μm	50%
weight	7.5 lbs	.35 μm	20%

Figure 2: CCD photometry equipment used at the SJU observatory from *Photometry Lab Manual* p. 32

Programs/Software:

The Sky X Professional (TheSkyX)

The Sky X Professional was the software used to control the camera's viewing direction when collecting data.

CCDops

CCDops was the software used to control the camera's functions that create/save CCD frames.

The typical commands are: set the temperature (cooling) of the CCD, focus, grab images (exposure time for flat, dark, and object frames), examine images (histogram), save images (.fit format), and reduce images by dark-subtraction, flat-fielding, or averaging.

Gaia

Gaia was the software used for reduced-frame analysis; determining the instrumental magnitudes from flat fielded, dark corrected images.

Initialization:

On a no-visible-clouds night, the programs CCDops and The Sky X Professional were initialized. Through TheSkyX, comlink was established between the mount and the program allowing control of the movement motors. In CCDops the camera temperature was set to -20°C where a thermoelectric cooler cooled the temperature of the KAF-1001E. In TheSkyX a spot in the sky, free of bright stars, was selected. CCDops was used to auto-grab flat frame images of pre-sunset blue sky. When the sky darkened enough to produce unsaturated images (saturation value close to 60,000 ADU's) with the shortest possible exposure (.12 sec) flat frames were ready to be collected.

Flat Frames:

Individual pixels have different sensitivities to light. If left uncorrected, they would be a prominent source of uncertainty ($\sim 5\%$). The solution to this issue is taking a picture of a uniformly illuminated surface, and record the count in each pixel. Evidently, this 'flat frame' count records how each pixel responds to one particular flux level. Thus to correct for the different sensitivities in the pixels we just divide (pixel by pixel) the raw CCD frame by the recorded flat frame. Here an assumption is made that the small section of a blue sky covered by the CCD frame is uniform.

After sunset, when the sky is dim enough to avoid saturation in short (< 1.5 sec) exposures, an

apparent no-stars spot was chosen using The Sky X Professional program. Flat frames images were grabbed using CCDops once a reasonable histogram was achieved (close to 60,000 ADU's) with a starting exposure time of approximately 0.12 seconds for the B filter. Three images were grabbed from each of the main filters at this spot; the exposure times were increased as necessary to retain a reasonable histogram. Once three images from each of the four main filters was attained, this process was then repeated for a different apparent dark spot in the sky. Flat frame sets were taken until approximately 1-1.5 second exposures were required for fully exposed images. At this point the sky would be too dim and thus stars would start to show through in the flat frames. For each filter at least three sets of three flat frames were collected each night and possibly more if time permitted.

Dark Frames:

Even in the total absence of light, pixels slowly accumulate charge due to electric current leaking. Electric current leaking is strongly influenced by temperature, which produces the accumulated charge in the absence of starlight, hence the name 'dark current'. To correct for these dark currents, the STL-1001E uses a thermoelectric cooler, which can cool the CCD below the surrounding temperature. Here the STL-1001E was cooled to -20°C, which reduced the dark currents by more than a factor of 10, however the dark currents are still not negligible for long exposures. To correct for these dark currents, 'dark frames' were taken. A dark frame is an exposure with the shutter closed as to see the 'hot pixels', which are the pixels that have large dark currents. The dark frames can be subtracted from an equally timed exposed from to correct for the non-photon induced current.

Once the flat frames were taken, dark frames were taken using CCDops at different exposure lengths. Three dark frames were auto grabbed for each of the following exposure times 300,

120, 60, 30, and 15 seconds. These different exposure lengths corresponded to the predetermined exposure lengths that would be used for the IC4665 open cluster and our target star, ASAS182612, which is the main focus of this thesis.

Focus:

The aim of 'focus' is to achieve the smallest possible Full Width at Half Maximum (FWHM) of the desired stars. At this point each star's light is concentrated in the smallest possible number of pixels. The fewer number of pixels used for the object yields relatively less noise in the stellar magnitude because each pixel has a certain 'background noise'.

After the dark frames were collected, any dim star (~4 or 5 magnitude) was found using The Sky X Professional and brought into the focus mode in CCDops. The focus, with a refresh time of 0.1 seconds, was adjusted to achieve the peak count in the frame on the focuser. At this point the telescope's focus was best calibrated for the current atmospheric conditions.

IC4665 CCD Frames for Calibration:

Following the focusing of telescope, the telescoped was directed to the open cluster IC4665. This particular cluster has well known values for the magnitudes of the stars and in Figure 3 the stars of interest, 24, 29, 21, 27, 23, 31, 32, and 33, are displayed. The stars of interest in the IC4665 cluster are used during the data analysis as a calibration tool to relate the instrumental magnitudes to their accepted magnitudes.

Using the focus mode to pan the telescope, the telescope was centered on a location where the stars of interest were in view. CCD images were then grabbed of the open cluster cycling through the B, V, R, and I filters. Three images with each of the designated filters were

collected. For exposures of less than 15 seconds, the object frames were automatically dark-subtracted rather than using the previously collected dark frames. The term 'object frame' refers to the raw CCD frame of the sky grabbed by the camera-controlling software.

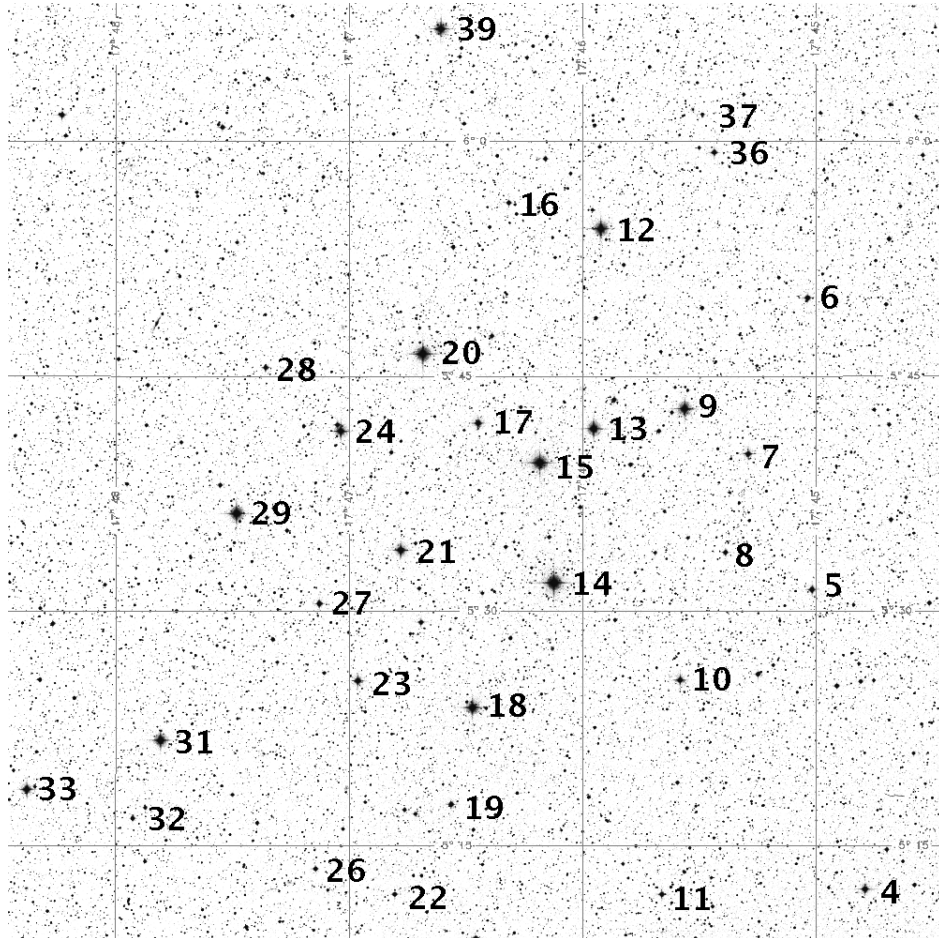


Figure 3: IC4665 open cluster star chart from <http://www.physics.csbsju.edu/ccd/ic4665ba.gif>

ASAS182612 CCD Frames:

After the IC4665 images had been collected, the telescope was moved to locate the star of interest, ASAS182612, near the star KU Her. Using the focus mode to pan the telescope, the telescope was centered on the star ASAS182612 as seen in Figure 4 with other stars of interest in view. CCD images were then grabbed of the star and surrounding stars of interest from each

of the main filters B, V, R, and I. Three images with each of the main filters were collected. For exposures of less than 15 seconds, the object frames were automatically dark-subtracted.

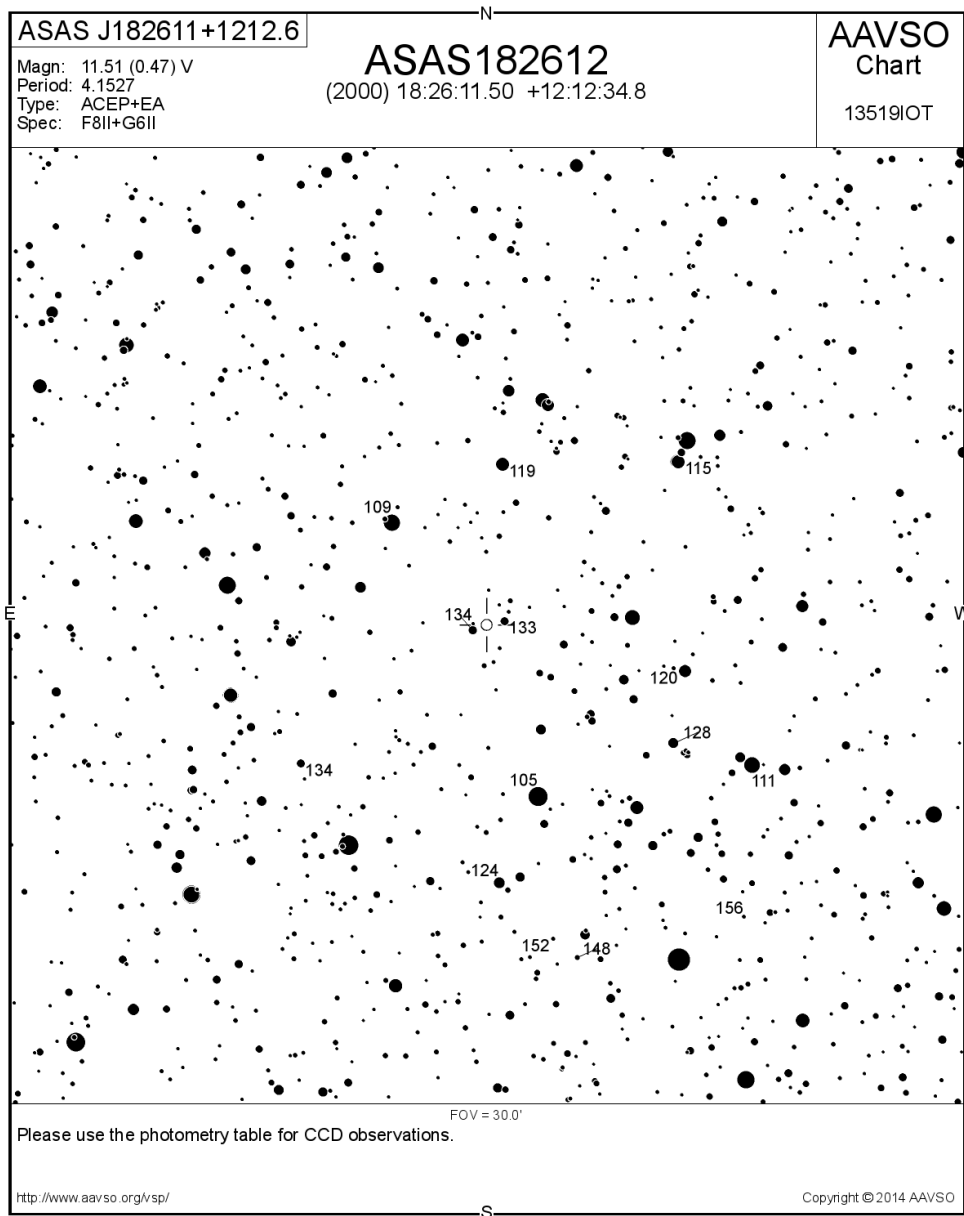


Figure 4: ASAS182612 star chart from <http://www.physics.csbsju.edu/ccd/182612b.png>

Data Frames:

After the data collection process, through CCDops, the flat frames were averaged for each individual set of three images for each of the main filters (B, V, R, or I) for the varying locations

in the sky. Next the three averaged flat frames, for a specific filter, were then compared to one another by flat-fielding the averaged flats with each other. The best flat field set was then selected. A single peaked histogram of the resulting image with no trends was an excellent indicator of a good flat set unless stars were visible in the frame. The final flat frames were used for flat-field correction of the object frames.

In CCDops, the median of the three Dark frames for the exposure times 300, 120, 60, 30, and 15 seconds were collected. These median Dark frames were used for dark-subtraction of the object frames.

The object frames of the IC4665 open cluster and ASAS182612 were converted into 'reduced frames'. The reduced frames were where the object frame had been both dark-subtracted and flat field corrected. For CCD frames that were already dark-subtracted only the flat-field correction needed to be applied. By converting the object frames into reduced frames, the reduced frames contain the actual distribution of photons where the adjustments for non-photon induced charge and varying pixel sensitivity have been corrected.

4 Data/Analysis

Gaia Collection of Star Magnitudes:

From the reduced frames, the magnitudes of the stars, 24, 29, 21, 27, 23, 31, 32, and 33, in Figure 3 of the IC4665 open cluster frame and the target stars in Figure 4 of the ASAS182612 frame were collected using the Gaia software.

Once a reduced frame was opened in Gaia, under the View tab, the color scale algorithm was set to histogram equalization, which made the stars more prominent in the reduced frames. Under the Image-Analysis tab, Aperture photometry was selected with the subsection Results in magnitudes were the parameters were set as described in the Photometry Lab Manual for data collection. Next, the define object aperture function was used to select the stars of interest in the reduced frame. Once all the stars were selected, the calculate results function was used to compute the magnitudes of the defined stars and the values were recorded.

This process was repeated for all of the reduced frames of B, V, R, and I filters of the IC4665 open cluster and ASAS182612.

Color Correction:

The magnitudes of the IC4665 and ASAS182612 stars in the B, V, R, and I filters were converted into the color indices, the ratio measuring the relative amounts of two colors. The following indices (B-V) vs. (b-v), (v-V) vs. (B-V), (R-I) vs. (r-i), and (i-l) vs. (R-I) were plotted to determine the linear fit color correction equation for the (B-V), (R-I), (v-V), and (i-l) indices of the form:

$$f(x) = a + bx \quad (16)$$

Since the magnitudes of the B, V, R, and I filters were known for the target stars in IC4665, the color correction process was first done for the IC4665 magnitudes. The median slopes of the IC4665 fit equations were used for each respective index (only adjusting a) when fitting the ASAS182612 indices. Once plotted, the linear fit served as a correction equation for ASAS182612 indices.

Download AAVSO ASAS182612 Magnitude Data:

Several years (6/08/2007-10/18/2014) of data of the measured magnitude of ASAS182612 were downloaded from the American Association of Variable Star Observers (AAVSO) at aavso.org. This data from AAVSO was used for comparison with the SJU values.

Condense AAVSO Data:

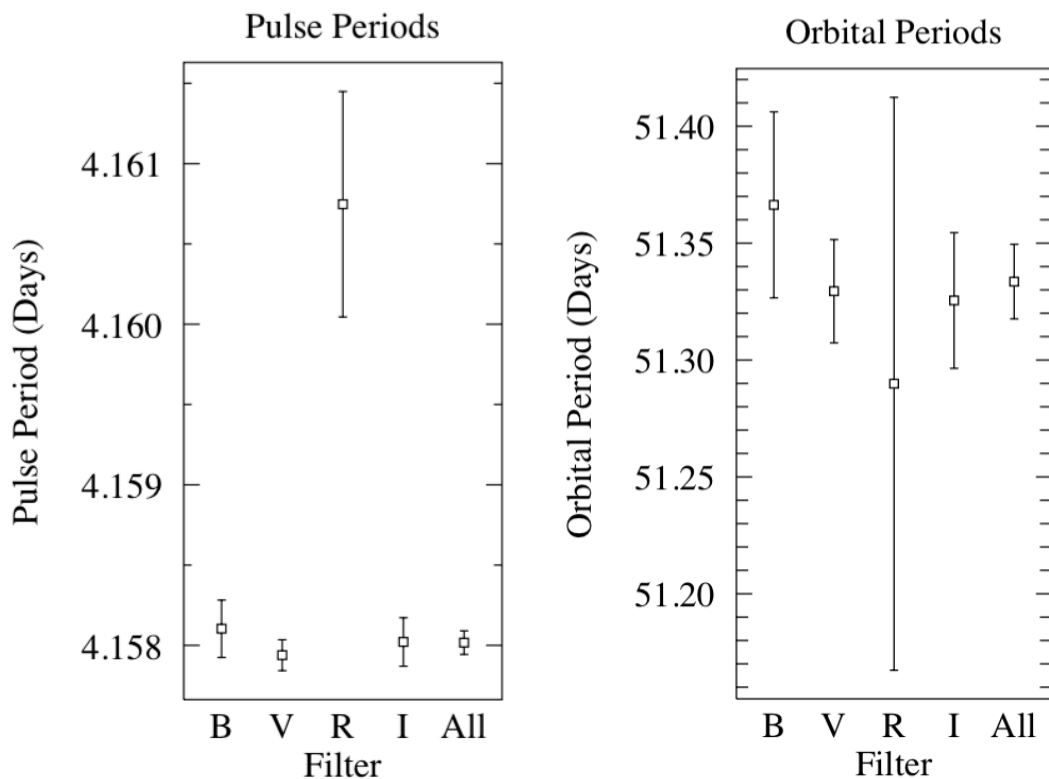
The downloaded data from AAVSO contains the Julian Day, magnitude, filter, and initials of the observer of each observation made on ASAS182612. The data was sorted by Julian day and then into four separate files for the B, V, R, and I filters. Running the program `RemoveDups.f` on each of the four separate files condensed the data from its original state by averaging the magnitudes and Julian day fractions for observations made by the same observer on the same Julian day. The program also subtracts of 2454300 from the averaged Julian Days.

Mathematica Chauvenet Criteria and Fit Functions on AAVSO Data:

Once the AAVSO data was condensed, the data still needed to be further reduced by removing outlying data points. The application of Chauvenet's criterion, assessing whether one piece of experimental data from a set of observation is likely to be an outlier, was applied to each of the condensed data sets for the B, V, R, and I magnitudes using Mathematica code to remove the spurious points.

After the outlier points were removed from the data set, the corrected data was then subjected to a truncated Fourier series non-linear fit. From the non-linear fit, the best-fit parameters and the parameter confidence intervals of the fit displayed the pulse and orbital frequencies and their corresponding confidence intervals for ASAS182612.

From the pulse and orbital frequencies of each of the main filters, the pulse and orbital periods were calculated. The multiple main filter values for the pulse and orbital periods were then used to obtain weighted average pulse and orbital periods. Using the plot program in terminal, plots were created of the pulse (Figure 5) and orbital (Figure 6) periods consisting of the B, V, R, I, and composite filters. At this point, the pulse period was assumed to be unchanging because of the relatively constant pulse periods from the multiple filters.



Figures 5 & 6: Pulse and orbital periods of ASAS182612 from AAVSO data

AAVSO Pulse and Orbital Periods:

The truncated Fourier series non-linear fit was used to plot the corresponding B, V, R, and I magnitudes vs. Julian day with a modulus to display the full pulse and orbital periods. The AAVSO V filter data is shown below in Figure 7 and Figure 8.

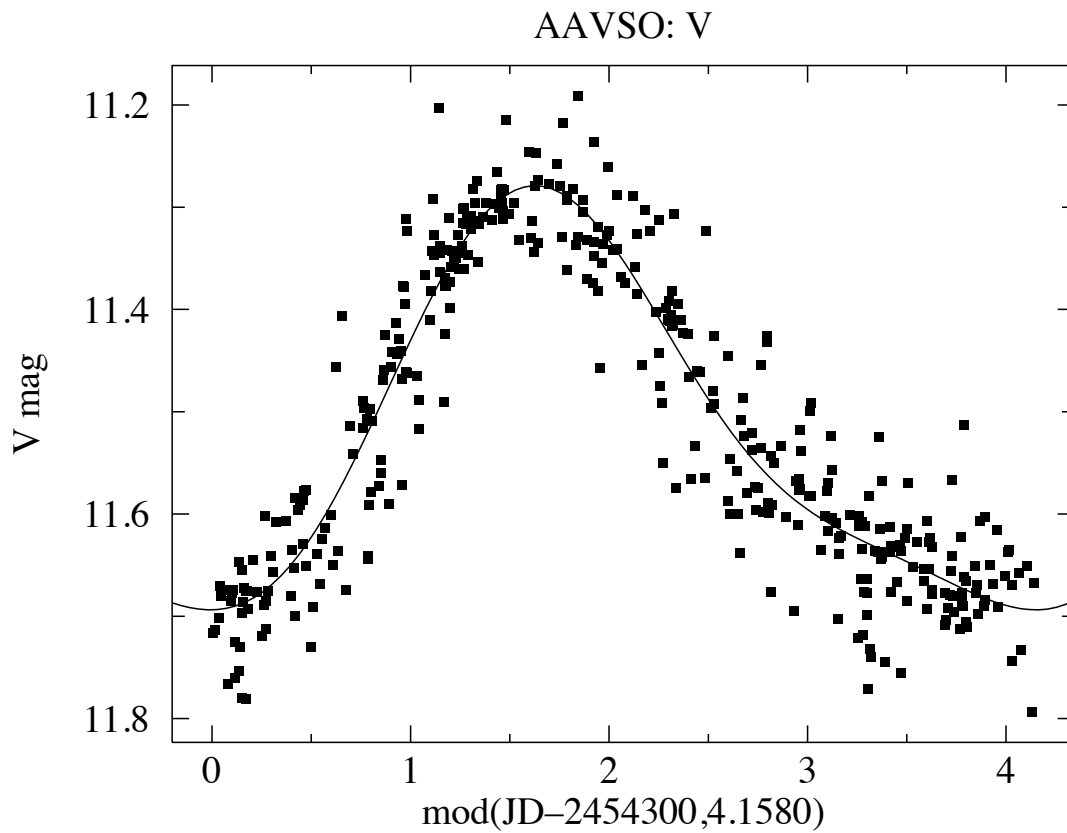


Figure 7: Wrapped plot of the measured V magnitude vs. pulse period of ASAS182612 from AAVSO data

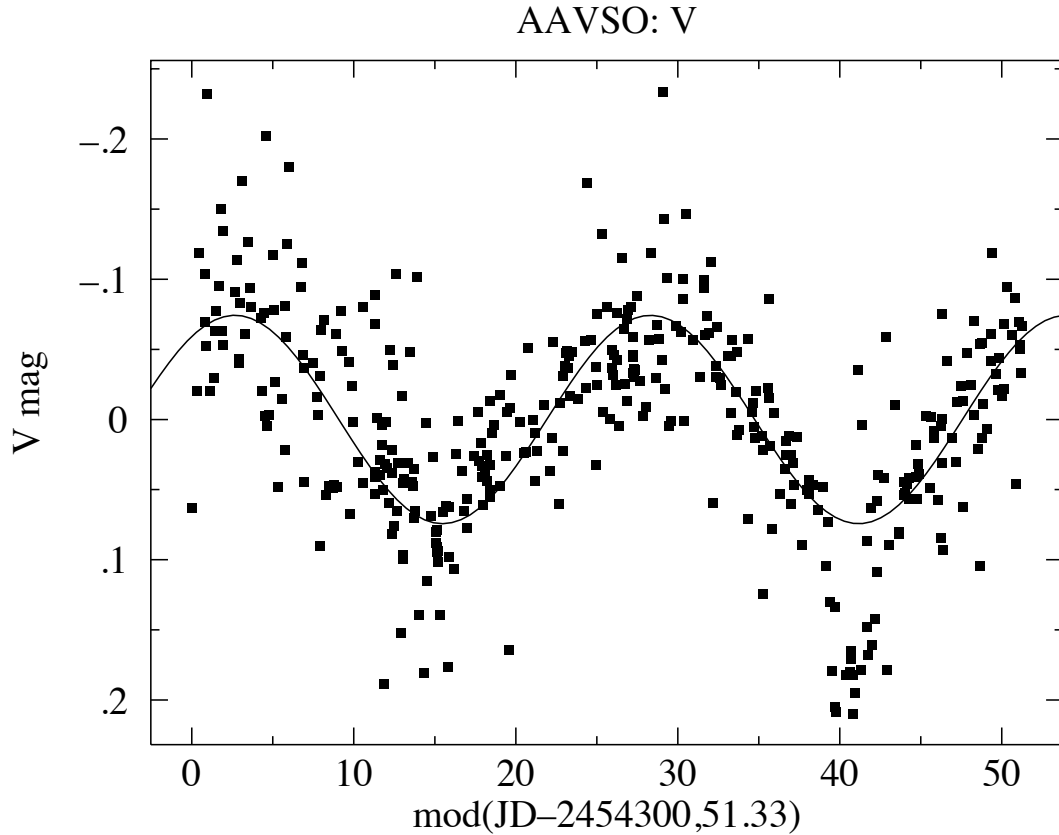


Figure 8: Wrapped plot of the measured V magnitude vs. orbital period of ASAS182612 from AAVSO data

Download SJU ASAS182612 Magnitude Data:

Several years (2007-2014) of data of the measured magnitude of ASAS182612 was downloaded from the SJU Observatory data files at <http://www.physics.csbsju.edu/thesis/>. This data, in addition to recently recorded data (7/9/14-10/23/14), was used for calculation of the pulse period, orbital period, and angular acceleration of the pulse period as viewed from the SJU Observatory.

Mathematica Fit Functions with Angular Acceleration on SJU Data:

The SJU data was subjected to a truncated Fourier series non-linear fit with an additional

acceleration term, which will be referenced later. The best-fit parameters and parameter confidence intervals of the non-linear fit yielded the pulse and orbital frequencies along with their respective confidence intervals for ASAS182612.

Similar to the AAVSO data, the pulse and orbital periods of the star were calculated. The B, B-V, R-I, and I filter values for the pulse and orbital periods were used to obtain a weighted average pulse and orbital period. From the plot program in terminal, plots were created of the pulse (Figure 9) and orbital (Figure 10) periods of the filters and weighted average.

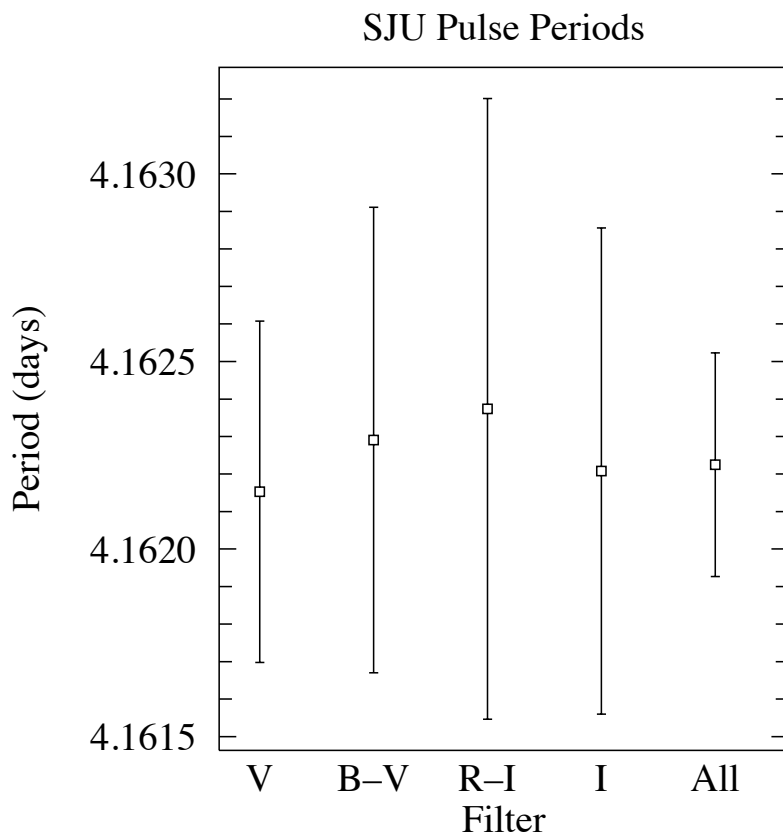


Figure 9: Pulse period of ASAS182612 from SJU data

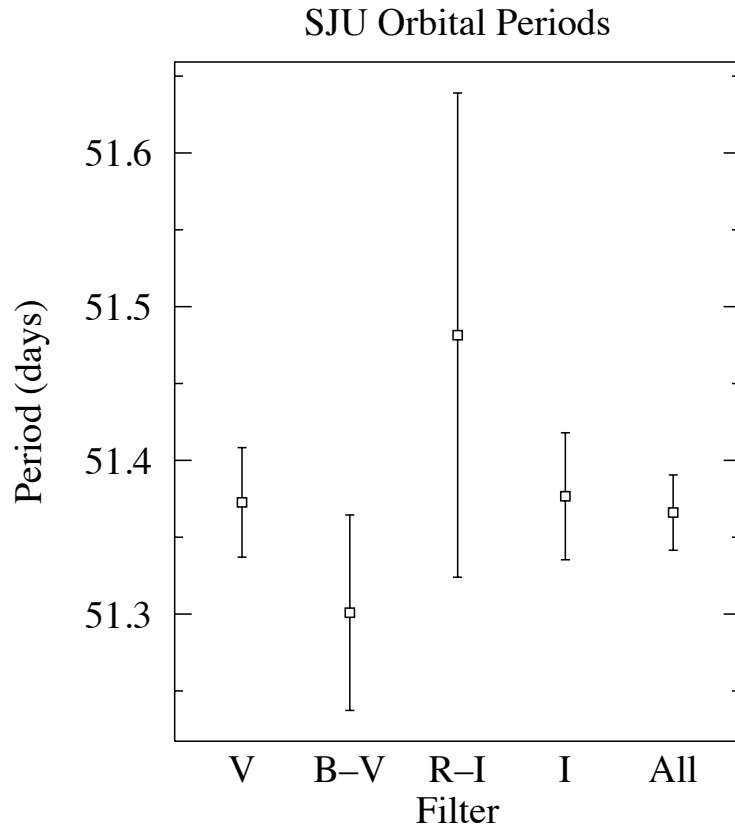


Figure 10: Orbital period of ASAS182612 from SJU data

SJU Pulse and Orbital Periods:

The truncated Fourier series non-linear fit was used to plot the corresponding B, B-V, R-I, and I magnitudes vs. Julian day with a modulus to display the full pulse and orbital periods. The SJU V filter data is shown below in Figure 11 and Figure 12.

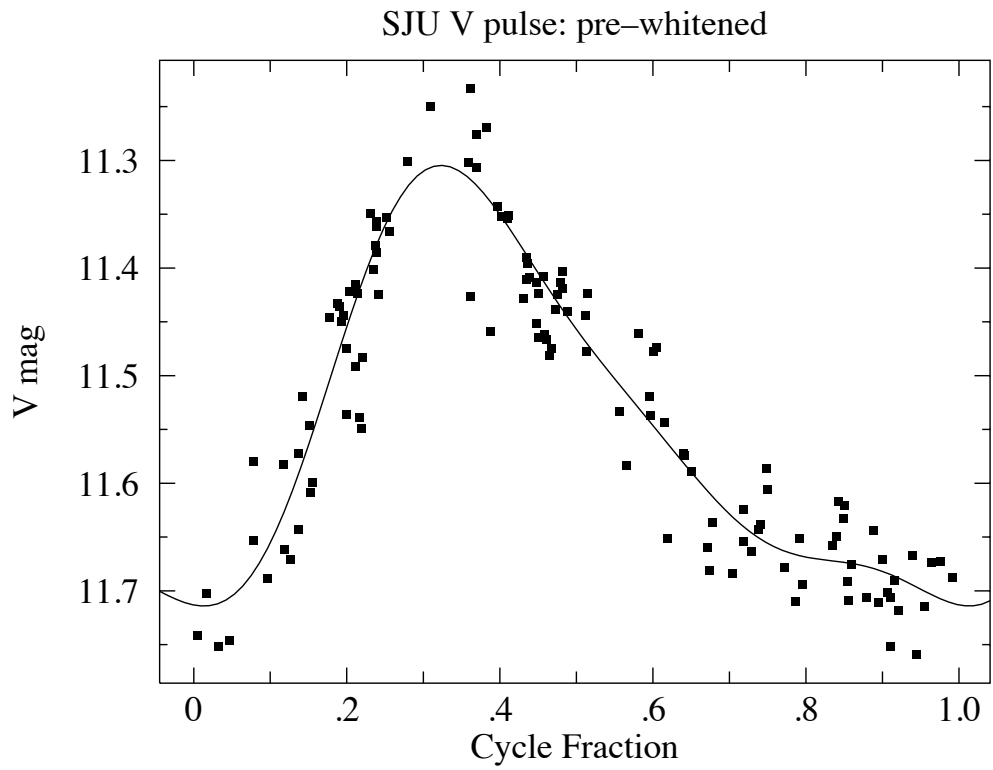


Figure 11: Wrapped plot of the measured V magnitude vs. pulse period of ASAS182612 from SJU data

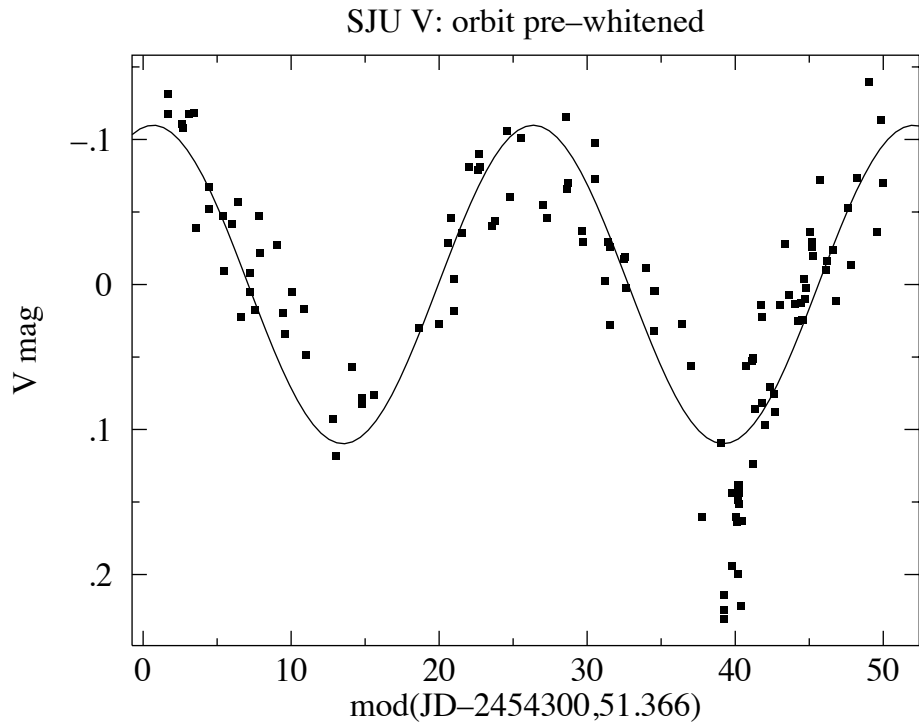


Figure 12: Wrapped plot of the measured V magnitude vs. orbital period of ASAS182612 from SJU data

SJU Angular Acceleration of the Pulse Period:

The truncated Fourier series acceleration term $K3 * x^2$ used in the equation

$$f(x) = k1 + k2 \sin(a(x + K3 * x^2)) + k3 \cos(a(x + K3 * x^2)) + k4 \sin(2a(x + K3 * x^2)) + k5 \cos(2a(x + K3 * x^2)) + k6 \sin(3a(x + K3 * x^2)) + k7 \cos(3a(x + K3 * x^2)) + k8 \sin(4a(x + K3 * x^2)) + k9 \cos(4a(x + K3 * x^2)) + K1 \sin(bx) + K2 \cos(bx) \quad (17)$$

provided values for each of the corresponding V, B-V, R-I, and I filters. The best-fit parameter for the acceleration term (K3) with the parameter confidence interval for each of the filters was plotted using the plot program in terminal (see Figure 13). The B, B-V, R-I, and I filter values for the acceleration term were used to obtain a weighted average acceleration term.

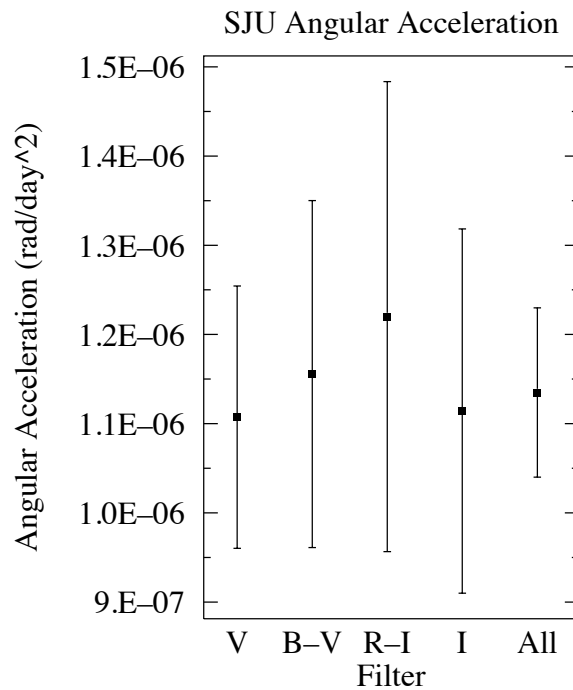


Figure 13: Plot of the angular acceleration in the pulse period of ASAS182612 from SJU data

Missing Light of ASAS182612:

The unseen light of the binary system was found by determining eclipse points in Figure 12. The eclipse points were chosen as the group of six points, which displayed large deviations ($>.05$ mag) from the orbital fit equation approximately 40 days into the cycle. For these eclipse points, the V magnitudes and B-V magnitudes were used to find the unseen light (magnitude) for B-V. With the expected magnitude for B-V already known, the unseen light was calculated for the B and V magnitudes through the equations:

$$V_{unseen} = -2.5 \log_{10} \left(10^{-\frac{V_{expected}}{2.5}} - 10^{-\frac{V_{seen}}{2.5}} \right) \quad (18)$$

$$B_{unseen} = -2.5 \log_{10} \left(10^{-\frac{B_{expected}}{2.5}} - 10^{-\frac{B_{seen}}{2.5}} \right) \quad (19)$$

The difference of $B_{unseen} - V_{unseen}$ yielded the total unseen light during the eclipses. From here a plot was made to display the relationship between the Unseen (B-V) and the Expected (B-V) as shown in Figure 14.

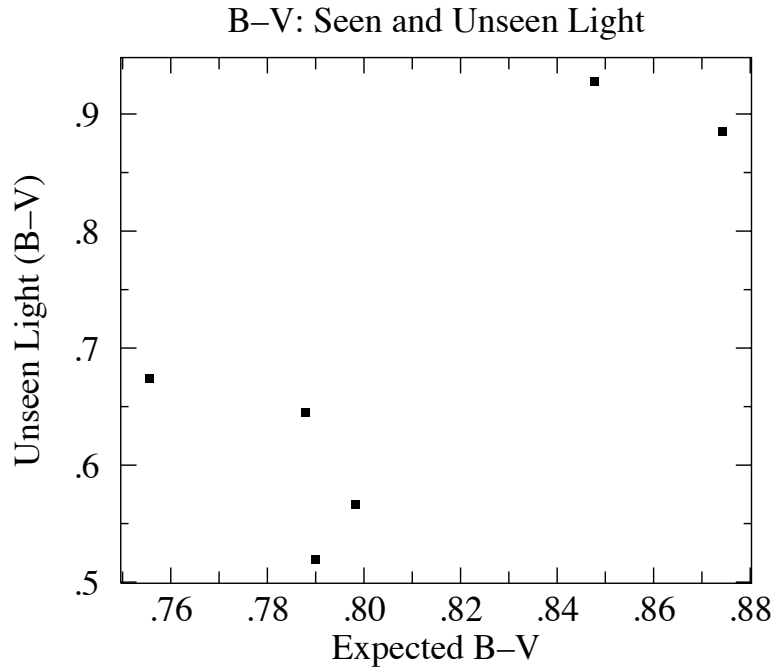


Figure 14: Plot of the unseen light vs. expected light of ASAS182612 during eclipses in the orbital period from SJU data

While the error bars for Figure 14 are large but not yet precisely determined, it appears that the eclipsed light is varying in temperature. This seems to suggest that the Cepheid is the eclipsed component. However, more work is needed to consider this a confident conclusion.

5 Conclusions:

From our analysis from 2007 to 2014, using B, V, R, and I filters, of the Type II Cepheid, eclipsing variable, ASAS182612, we determined the pulsation and orbital periods to be $4.1622 \pm .0003$ days and $51.366 \pm .025$ days, respectively. The angular acceleration of the pulse period was determined to be $(1.1 \pm .1) \times 10^{-6}$ rad/day².

Acknowledgements:

A special thank you is given to Dr. Thomas Kirkman, my thesis advisor, who helped with support and configuration of this thesis project. An additional thanks goes out to the Physics Department of Saint John's University for the contribution of supplying the tools for the project and analysis

References:

Bibliography

- 1) Percy, J. R. (2007). *Understanding variable stars*. Cambridge: Cambridge University Press.
- 2) Alcock, C., Allsman, R. A., Alves, D. R., Becker, A. C., Bennett, D. P., Cook, K. H., . . . Collaboration, M. (2002). The MACHO project Large Magellanic Cloud variable star inventory. XII. Three Cepheid variables in eclipsing binaries. *Astrophysical Journal*, 573(1), 338-350. doi: 10.1086/340560
- 3) Antipin, S. V., Sokolovsky, K. V., & Ignatieva, T. I. (2007). TYC 1031 01262 1: the first known galactic eclipsing binary with a type II cepheid component. *Monthly Notices of the Royal Astronomical Society*, 379(1), L60-L62. doi: 10.1111/j.1745-3933.2007.00335.x
- 4) Antonello, E. (2002). The effects of blending on the light curve shape of Cepheids. *Astronomy & Astrophysics*, 391(2), 795-799. doi: 10.1051/0004-6361:20020897
- 5) Feast, M. W., Laney, C. D., Kinman, T. D., van Leeuwen, F., & Whitelock, P. A. (2008). The luminosities and distance scales of type II Cepheid and RR Lyrae variables. *Monthly Notices of the Royal Astronomical Society*, 386(4), 2115-2134. doi: 10.1111/j.1365-2966.2008.13181.x
- 6) Schmidt, E. G., Johnston, D., Langan, S., & Lee, K. M. (2005). Photometry of type II Cepheids. III. The intermediate-period stars. *Astronomical Journal*, 130(2), 832-841. doi: 10.1086/431176
- 7) Templeton, M. R., & Henden, A. A. (2007). Multicolor photometry of the type II Cepheid prototype W Virginis. *Astronomical Journal*, 134(5), 1999-2005. doi: 10.1086/522945
- 8) Kirkman, Thomas. *Photometry Lab Manual*. Lab handbook. St. John's University. Collegeville, MN. 2007. Photometry.pdf.